Wang et al. *Zool. Res.* 2024, 45(3): 567−574
https://doi.org/10.24272/j.issn.2095-8137.2024.026

ZR | Zoological Research

Article Open Access

Improvement in Tol2 transposon for efficient large-cargo capacity transgene applications in cultured cells and zebrafish (*Danio rerio*)

Peng-Cheng Wang[1,2], Hao Deng[2,3], Rang Xu[4,*], Jiu-Lin Du[2,5,6,*], Rongkun Tao[2,*]

[1] *Department of Pediatric Cardiology*, *Xinhua Hospital*, *Shanghai Jiao Tong University School of Medicine*, *Shanghai* 200092, *China*
[2] *Institute of Neuroscience*, *State Key Laboratory of Neuroscience*, *Center for Excellence in Brain Science and Intelligence Technology*, *Chinese Academy of Sciences*, *Shanghai* 200031, *China*
[3] *Medical School*, *Kunming University of Science and Technology*, *Kunming*, *Yunnan* 650500, *China*
[4] *Scientific Research Center*, *Xinhua Hospital*, *Shanghai Jiao Tong University School of Medicine*, *Shanghai* 200092, *China*
[5] *University of Chinese Academy of Sciences*, *Beijing* 100049, *China*
[6] *School of Life Science and Technology*, *ShanghaiTech University*, *Shanghai* 200031, *China*

ABSTRACT

Most viruses and transposons serve as effective carriers for the introduction of foreign DNA up to 11 kb into vertebrate genomes. However, their activity markedly diminishes with payloads exceeding 11 kb. Expanding the payload capacity of transposons could facilitate more sophisticated cargo designs, improving the regulation of expression and minimizing mutagenic risks associated with molecular therapeutics, metabolic engineering, and transgenic animal production. In this study, we improved the Tol2 transposon by increasing protein expression levels using a translational enhancer (*QBI SP163*, ST) and enhanced the nuclear targeting ability using the nuclear localization protein H2B (SHT). The modified Tol2 and ST transposon efficiently integrated large DNA cargos into human cell cultures (H1299), comparable to the well-established super PiggyBac system. Furthermore, mRNA from ST and SHT showed a significant increase in transgene delivery efficiency of large DNA payloads (8 kb, 14 kb, and 24 kb) into zebrafish (*Danio rerio*). This study presents a modified Tol2 transposon as an enhanced nonviral vector for the delivery of large DNA payloads in transgenic applications.

Keywords: Zebrafish; Tol2 transposase; Transgene; Large payload; Synthetic biology

INTRODUCTION

Genetic engineering, particularly the integration of large DNA payloads, plays a pivotal role in transgenic animal model production, gene therapies, cell-based therapies, and biosynthetic applications (Mashel et al., 2020; Zhang et al., 2023). The challenges associated with efficiently integrating large DNA payloads exceeding 11 kb into host genomes have driven the exploration of various novel tools and approaches.

In the field of transgene tools, transposons—mobile DNA segments capable of changing their positions within the genome—have emerged as promising non-viral vehicles for the delivery of large DNA cargos. Notably, the medaka fish Tol2 transposon, which exhibits high transposition efficiency and a cargo capacity of up to 11 kb, has shown activity across various vertebrates (Balciunas et al., 2006; Kawakami, 2007; Urasaki et al., 2008). In contrast, other widely used transposons such as Sleeping Beauty (SB) or PiggyBac (PB), though optimized for transferring foreign DNA into cell cultures and animals, are limited by relatively modest cargo capacity of ~8 kb and are prone to overexpression inhibition (Balciunas et al., 2006; Sandoval-Villegas et al., 2021). Additionally, viral vectors such as adeno-associated viruses (AAVs) and lentiviruses present payload limitations and safety concerns regarding genotoxicity and immunogenicity (Tambuyzer et al., 2020). Meganucleases, such as I-SceI, exhibit limitations in terms of genome engineering stability and efficiency due to challenges in maintaining activity over extended periods (Grabher et al., 2004; Silva et al., 2011). Moreover, although CRISPR-Cas9 is recognized as a revolutionary and precise genome editing tool that employs guided RNA molecules to target specific DNA sequences, it encounters difficulties in efficiently integrating large DNA donors due to off-target

Received: 22 March 2024; Accepted: 26 April 2024; Online: 28 April 2024
Foundation items: This work was supported by the National Science and Technology Innovation 2030 Major Projects (2021ZD0202200), National Natural Science Foundation of China (32171090, 81970264), Shanghai Science and Technology Commission (21ZR1482600), and 2023 Youth Innovation Promotion Association CAS
*Corresponding authors, E-mail: forestdu@ion.ac.cn; rangxu@shsmu.edu.cn; rktao@ion.ac.cn

effects and variable expression levels of Cas9 and single-guide RNA (sgRNA) (Bak & Porteus, 2017; Li et al., 2015; Yuen et al., 2017). As such, the Tol2 transposon is an attractive candidate for overcoming the limitations posed by other systems.

In this study, we implemented strategies to increase Tol2 protein expression levels and enhance nuclear targeting and explored the potential of Tol2 as an alternative non-viral vector for transgenic applications in cell cultures. We also investigated the enhanced capabilities of the modified Tol2 transposon in facilitating the integration of large payloads, including tissue-specific expression constructs and the complete luciferin synthetic pathway in zebrafish (*Danio rerio*) (Mitiouchkina et al., 2020). Collectively, this study identified the modified Tol2 transposon as a promising candidate for transgene applications.

MATERIALS AND METHODS

Plasmid design and construction

All polymerase chain reaction (PCR) experiments utilized PrimeSTAR Max DNA Polymerase (TaKaRa, Japan). Plasmids were constructed using the Gibson assembly approach for seamless cloning. For the Tol2-EGFP constructs, we obtained the backbone by inverted PCR (P1–P2) and amplified the Tol2 transposase using primers (P3–P4) with 16 base pairs homologous to the linearized vector. The cDNA for the translational enhancer *QBI SP163* was synthesized by GENEWIZ (Azenta Life Sciences, China) and fused at the N-terminal of the Tol2 transposase (P5–8). To increase the nuclear localization of the Tol2 transposase, histone *H2B* was amplified and inserted between Tol2 and the *SP163* enhancer (P9–12). To create plasmids for *in vitro* transcription of Tol2 mRNA, a strong prokaryotic *T0* terminator was annealed and inserted in front of the *BGH* terminator of the *pcDNA3.1-Tol2* vectors without enhanced green fluorescence protein (EGFP) (P13–16). Tol2 was replaced to construct the super PiggyBac (sPB) transposase plasmid (P17–20). The cDNA for βactin-cyto-mCherry-GRIT was amplified from *pminiTol2-βactin-cyto-mCherry-GRIT* (Tao et al., 2023) and inserted into the sPB donor plasmid containing the sPB inverted terminal repeat (ITR) sequences (P21–24). The *pminiTol2-flk1* and *pminiTol2-eleva3* plasmids were digested with EcoRI/NotI and XhoI/NotI (Thermo Fisher Scientific, USA), respectively. The cDNA for H2B-mScarlet and NES-mCherry-PhoCl-NLS (Zhang et al., 2017) was amplified (P25–28) and ligated into the *pminiTol2-flk1* and *pminiTol2-eleva3* plasmids, respectively. To construct a plasmid carrying the whole synthetic bioluminescence pathway, all cDNA for the luciferin synthetic enzymes was synthesized by GENEWIZ using a *pminiTol2-10UAS* vector with a *E1B* promoter (Abdelfattah et al., 2019), followed by cloning into the *pTol2-βactin-Gal4-VP64* plasmid (Azenta Life Sciences, China). Both *pcDNA3.1-SP163-H2B-tol2-EGFP* and *pcDNA3.1-SP163-H2B-tol2-T0* were uploaded to GenBank (PP708881 and PP708882). The sequences of *SP163*, *H2B*, and *T0* terminator are shown in Supplementary Figure S1A, B. Primers and complete DNA sequences of plasmids used in this study are available in Supplementary File S1.

Cell culture and transfections

H1299 cells were sourced from the Cell Bank of the Chinese Academy of Sciences. The H1299 cells were cultured in RPMI-1640 medium (Thermo Fisher Scientific, USA) supplemented with 10% fetal bovine serum (FBS, ExCell Bio, China) and 1% penicillin/streptomycin (Thermo Fisher Scientific, USA) and maintained at 37°C in a 5% CO_2 environment.

For transient transfections, cells were seeded in a 96-well glass-bottomed dish (Cellvis, China) at 70% confluency. Co-transfections of donor plasmids and transposases with different ratios were carried out using Lipofectamine 3000 (Thermo Fisher Scientific, USA) following the manufacturer's protocols. The donor plasmids were consistently set at 0.1 μg/well with different amounts of transposase plasmids adjusted according to specified ratios. For cell clone counting, transfected cells were plated at a density of 1 000 cells/well in a 6-well plate and selected using 0.5 μg/mL puromycin for 10 days.

High content imaging

For H1299 cells transfected with different Tol2-EGFP plasmids, the RPMI-1640 medium was removed and replaced with 100 μL of 4% paraformaldehyde (PFA) for 30 min, followed by staining with 300 nmol/L 4',6-diamidino-2-phenylindole (DAPI) solution (Shangon Biotech, China) for 30 min and washing five times with phosphate-buffered saline (PBS, Mxbioscience LLC, China). Imaging was conducted using the Operetta CLS high-content imaging system (PerkinElmer, USA), employing a 10× objective and capturing fluorescence signals with the fluorescein isothiocyanate (FITC) and DAPI channels.

Flow cytometry

The H1299 cells were trypsinized, suspended in PBS with 10% FBS, and loaded into FACS tubes for analysis using a BD FACSAria™ Fusion Flow Cytometer (BD Biosciences, USA). In total, 20 000 events were counted for each sample, and data were recorded based on the forward (FSC) and side scatter (SSC) properties of the cells. Fluorescence emitted by each cell upon excitation with a 561 nm laser was collected to determine the positive ratio. All data were processed using FlowJo software.

In vitro transcription and mRNA purification

The mRNA preparation was performed using a T7 mMESSAGE mMACHINE kit (Invitrogen, USA) according to the manufacturer's manual (Tao et al., 2017). The cDNA for different Tol2 transposases containing the *CMV* promoter and *BGH* terminator was amplified by PCR, followed by the *in vitro* synthesis of large amounts of capped RNA at 37°C. The mRNA products were precipitated by lithium chloride incubation, diluted with diethylpyrocarbonate (DEPC)-treated nuclease-free water, and maintained at −80°C before microinjection.

Zebrafish husbandry

Adult zebrafish (*Nacre* line) were raised under standard laboratory conditions using an automatic fish housing system at the Center for Excellence in Brain Science and Intelligence Technology (Institute of Neuroscience) (Shanghai, China). The microinjection procedure was performed as described previously (Tao et al., 2023). In brief, a 1 nL mixture of plasmid DNA (12.5 ng/μL) and Tol2 mRNA (12.5 ng/μL) was injected into one-cell stage zebrafish embryos, which were maintained in egg water (5 mmol/L NaCl, 0.17 mmol/L KCl, 0.33 mmol/L $CaCl_2$, 0.33 mmol/L $MgSO_4$) at 28.5°C. At 4 days post-fertilization (dpf), the zebrafish larvae were anesthetized

in egg water containing 1 mmol/L tricaine (Sigma, USA) and positioned on an inverted fluorescent microscope (Olympus, Japan) to assess the number of red fluorescent cells using the Texas Red channel. All zebrafish experimental protocols were approved by the Chinese Academy of Sciences (approval No. NA-046-2019).

Excision PCR

Excision PCR was conducted according to previously described methods (Suster et al., 2009). After microinjection, zebrafish embryos were collected at 10 hours post-fertilization (hpf) and lysed in 0.2 mL PCR tubes with 50 μL of lysis buffer (10 mmol/L Tris-HCl, 10 mmol/L EDTA, 200 mg/mL proteinase K, pH 8.0), followed by incubation at 50°C for 3 h and enzyme inactivation at 95°C for 5 min. Routine PCR was performed using specifically designed primers 5'-CACACCCGCCG CGCTTAAT and 5'-GCGTCGATTTTTGTGATGCTCGT to amplify a DNA fragment approximately 770 bp in length, followed by agarose gel electrophoresis (1%).

The abundance of excision products was further quantified by quantitative real-time polymerase chain reaction (qPCR) using a Hieff qPCR SYBR Green Master Mix Kit (Yeasen, China) on the Roche LightCycler 480 (Roche, USA). Zebrafish β-actin was used as a control with the forward primer 5'-AAGCAGGAGTACGATGAGTC and reverse primer 5'-TGG AGTCCTCAGATGCATTG. The relative levels of excision product per embryo were calculated by normalizing to zebrafish β-actin.

***In vivo* imaging and bioluminescence detection**

Zebrafish larvae (4 dpf) were immobilized and embedded in 1.5% low melting agarose on a glass-bottom dish. All *in vivo* imaging experiments were conducted using an Olympus FV3000 upright confocal microscope under XLUMPlanFL N 10× water-immersion objective (N.A. 1.0) (Olympus, Japan). Red fluorescent protein (RFP) was excited using a 561 nm laser, and emissions ranging from 570–620 nm were captured by a photomultiplier tube (PMT) at a 3 μm axial step. The data were recorded in a 1 024×1 024 format at 12-bit depth. The 4 dpf zebrafish larvae carrying the synthetic luciferin pathway cargo were analyzed for bioluminescence detection, as described previously (Kotlobay et al., 2018). The zebrafish were exposed to egg water containing 0.1% dimethyl sulfoxide (DMSO) with or without caffeic acid (5 mmol/L) or hispidin (5 mmol/L) for 1 h, followed by luminescence recording using the 570–620 nm emission channel without excitation lasers. All data were processed using ImageJ software (NIH, USA). In brief, background subtraction was applied to the images, followed by projection of the image stacks and merging of the RFP and brightfield channels.

Statistical analysis

Images and data were presented either as a representative example of three independent experiments or as the mean values of at least three experiments. Data were represented as the mean±standard error of the mean (SEM). All statistical tests and graphs were performed using SigmaPlot (v.14.0) and GraphPad (v.9.0). Student's unpaired *t*-test (two-sided), one-way analysis of variance (ANOVA) test, and Chi-square test for trends were used to evaluate the significance of differences (*: P<0.05; **: P<0.01; ***: P<0.001; ****: P<0.0001). All figures were assembled using Adobe Illustrator 2020 (Adobe Systems, USA).

RESULTS

Improvement in Tol2 transposase with increased protein expression and nuclear targeting

The autonomous medaka Tol2 transposase, consisting of 649 amino acids (73.1 kDa), enables efficient integration of cargos up to 11 kb into the host genome via a cut-and-paste mechanism (Kawakami, 2007). While Tol2 has been widely utilized in transgene experiments with zebrafish, a thorough investigation of its intracellular expression levels and patterns has not yet been conducted.

In this study, we assessed the distribution and expression levels by fusing a modified Tol2 transposase with EGFP in cultured cells (Figure 1A). Our results revealed a low expression level of Tol2 in H1299 cells, likely due to the attenuated protein translation caused by the complex hairpin structure within the initial 300 nucleotides of Tol2 mRNA (Supplementary Figure 2A, B) (Kozak, 1986). Furthermore, we observed a moderate nuclear localization pattern of Tol2 (57.3%±2.2%) (Figure 1B), suggesting the presence of a monopartite nuclear localization signal (NLS) (LLFSPKRARLDTNNF) in the wild-type Tol2 protein, as predicted by cNLS Mapper (Kosugi et al., 2009). We modeled the 3D structure of Tol2 transposase using AlphaFold (Q9PVN3) to show the NLS position (Jumper et al., 2021) (Supplementary Figure S2C).

We posited that the transgene efficiency of Tol2 may be restricted by low protein expression levels and suboptimal nuclear targeting. To address these limitations, Tol2 expression was enhanced using the reported translational enhancer *QBI SP163* and nuclear localization efficiency was improved by fusing with the nuclear targeting protein H2B (Freeman et al., 2014; Stein et al., 1998). The *QBI SP163* translational enhancer resulted in a 3-fold increase in the number of positive cells and a 2-fold increase in the overall Tol2 expression level, accompanied by a minor decrease in nuclear localization (49.6%±1.4%) in the cells (Figure 1C, D; Supplementary Figure S2D, F). The incorporation of H2B eliminated the impact of complex hairpin structures at the start of the Tol2 coding sequence (CDS) (Supplementary Figure S2B). N-terminal H2B infusion led to an impressive 10-fold increase in total expression and a 13-fold higher nuclear EGFP signal, indicating that over 70% of Tol2 transposase was localized in the nuclei (Figure 1C, D; Supplementary Figure S2D, F). These strategies, aimed at overcoming the limitations associated with low protein expression and insufficient nuclear targeting ability in Tol2 transposase, may improve its utility in transgene applications.

Characterization of Tol2 transposition efficiency in cell cultures

Although Tol2 is widely used in vertebrates, its applications in cell cultures are not well-established (Huang et al., 2010; Tsukahara et al., 2015). To evaluate the transposition efficiency of the Tol2 and sPB systems in cell cultures, we co-transfected Tol2 transposase with a previously reported donor plasmid carrying a 9.4 kb cargo (*βactin-cyto-mCherry-GRIT*) at various ratios (Tao et al., 2023). After transfection, the cells underwent 10 days of puromycin selection, followed by cell clone counting and flow cytometry assessment (Figure 2A). Results showed that the efficiency of the Tol2 transposon system was comparable to the sPB system at higher transposase/donor ratios (1:10 to 1:50) (Figure 2B).

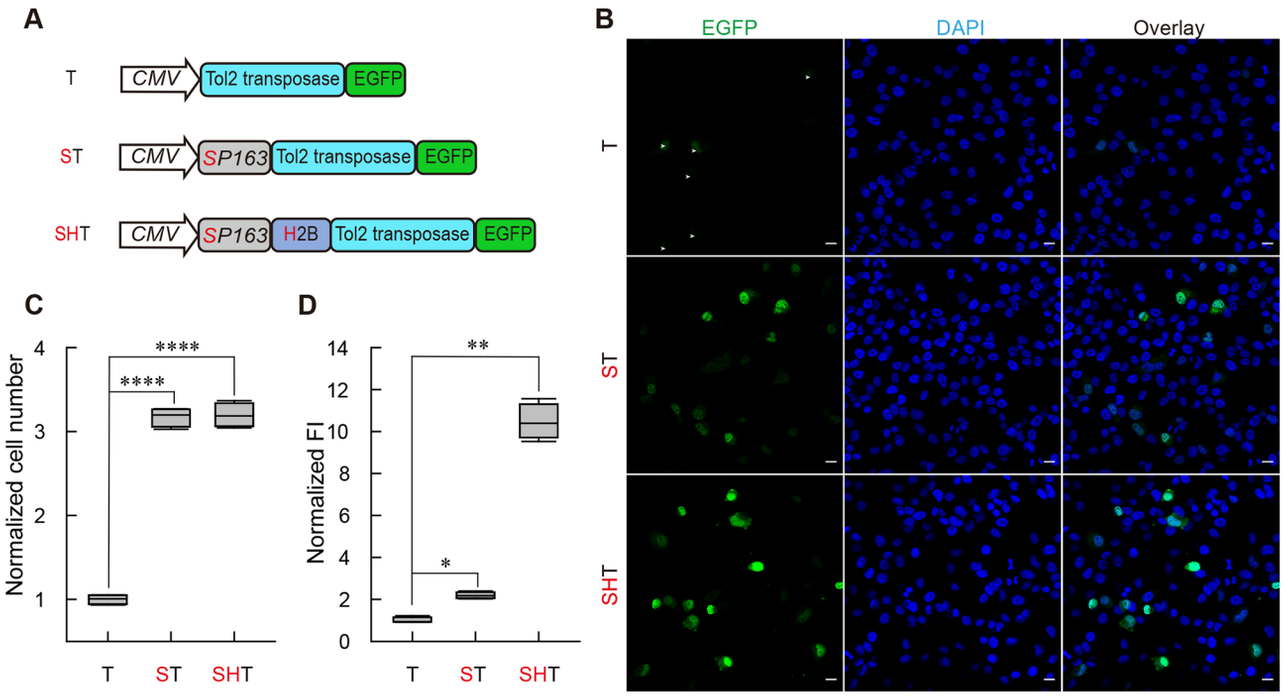

Figure 1 Design of improved Tol2 transposases with enhanced expression and nuclear targeting

A: Schematic of modified Tol2 transposase design. Tol2 transposase is driven by the *CMV* promoter and engineered for enhanced expression and nuclear targeting by incorporating the *QBI SP163* translational enhancer and *H2B*. B: Fluorescence microscopy images of H1299 cells transfected with EGFP-fused Tol2 transposase constructs: T (wild-type Tol2), ST (SP163-Tol2), and SHT (SP163-H2B-Tol2). Cells were fixed and stained with DAPI to visualize nuclei. Scale bars, 20 μm. C, D: Quantification of normalized EGFP fluorescence intensity in total cell cytosol (C) and nuclei (D). Data are mean±SEM. *n*=3 independent experiments. *: *P*<0.05; **: *P*<0.01; ***: *P*<0.001; ****: *P*<0.0001. Student's unpaired *t*-test.

Interestingly, Tol2 transposition efficiency was approximately 2-fold higher than that of the sPB system at lower ratios (1:250 to 1:31 250) (Figure 2B). Flow cytometry analysis also revealed similar transposition efficiencies for the T (wild type Tol2), ST, and sPB transposon systems at a transposase/donor ratio of 1:10 (Figure 2C). However, the SHT exhibited a higher cell mortality rate with a concomitantly low transposition efficiency, possibly due to prolonged high levels of nuclear transposase expression under the strong *CMV* promoter (Figure 2B). These findings highlight the potential utility of the T and ST transposon systems in cell culture applications.

Improved Tol2 transposon facilitates efficient transposition of large payload in zebrafish

We explored the performance of improved Tol2 mRNAs in zebrafish transgene experiments (Figure 3A) and assessed transposition efficiency using two donor plasmids of different sizes, as reported previously (Chiang et al., 2020). In brief, the F0 generation was divided into different groups based on the number of positive cells in individual fish (Figure 3B, E; Supplementary Figure S3A, B).

One donor plasmid, designated *pminiTol2-flk1-H2B-mScarlet*, carried an 8 kb payload that included a vascular-specific promoter, *flk1*, to direct the expression of nuclear RFP (H2B-mScarlet) within endothelial cells (Figure 3B). Single plasmid injection resulted in positive cell percentages of 19.66% for Group 2 and 3.42% for Group 3 (Figure 3C). When co-injected with wild-type Tol2 mRNA, these percentages increased to 27.88% and 7.69%, respectively (Figure 3C). Both ST and SHT significantly increased the number of positive cells in the F0 generation, reaching 30.91% and 33.15% for Group 2 and 16.36% and 24.46% for Group 3, respectively (Figure 3C). Additionally, we presented a more detailed comparison by further subdividing the groups using a histogram (Supplementary Figure 3A), which demonstrated the superior efficiency of ST and SHT compared to T.

The second donor plasmid, *pminiTol2-eleva3-NES-mCherry-PhoCl-NLS*, contained a substantial 14 kb payload that incorporated a neuronal-specific promoter, *eleva3*, designed to control the expression of a chimeric RFP within neuronal nuclei (Figure 3D). Injection of this donor plasmid, with or without wild-type Tol2 mRNA, yielded few positive cells in the 4 dpf zebrafish (2.67%, 0% for Group 2, 0.67%, 0% for Group 3) (Figure 3E). However, the inclusion of ST and SHT mRNA significantly increased the percentages to 22.04% and 30.4% in Group 2 and 11.02% and 14.4% in Group 3, respectively (Figure 3E). Additionally, the histogram with further subgroups also indicated higher efficiency for ST and SHT (Supplementary Figure 3B). Excision PCR analysis to detect the integration events mediated by different Tol2 transposases (Supplementary Figure 3C) demonstrated a higher number of integration events with ST and SHT at the molecular level for both donor plasmids (Supplementary Figure 3D, F). These findings are consistent with the observed positive cell numbers in larval zebrafish. Collectively, these experiments confirmed the superior performance of the enhanced ST and SHT transposons in facilitating DNA transgenesis in zebrafish, especially for large DNA payloads.

SHT mRNA enables whole luciferin metabolic pathway integration into zebrafish

An expanded transposon donor vector cargo capacity could accommodate multiple cistrons and gene circuits crucial for applications in metabolic engineering, such as the synthetic bioluminescence pathway. Bioluminescence, characterized by

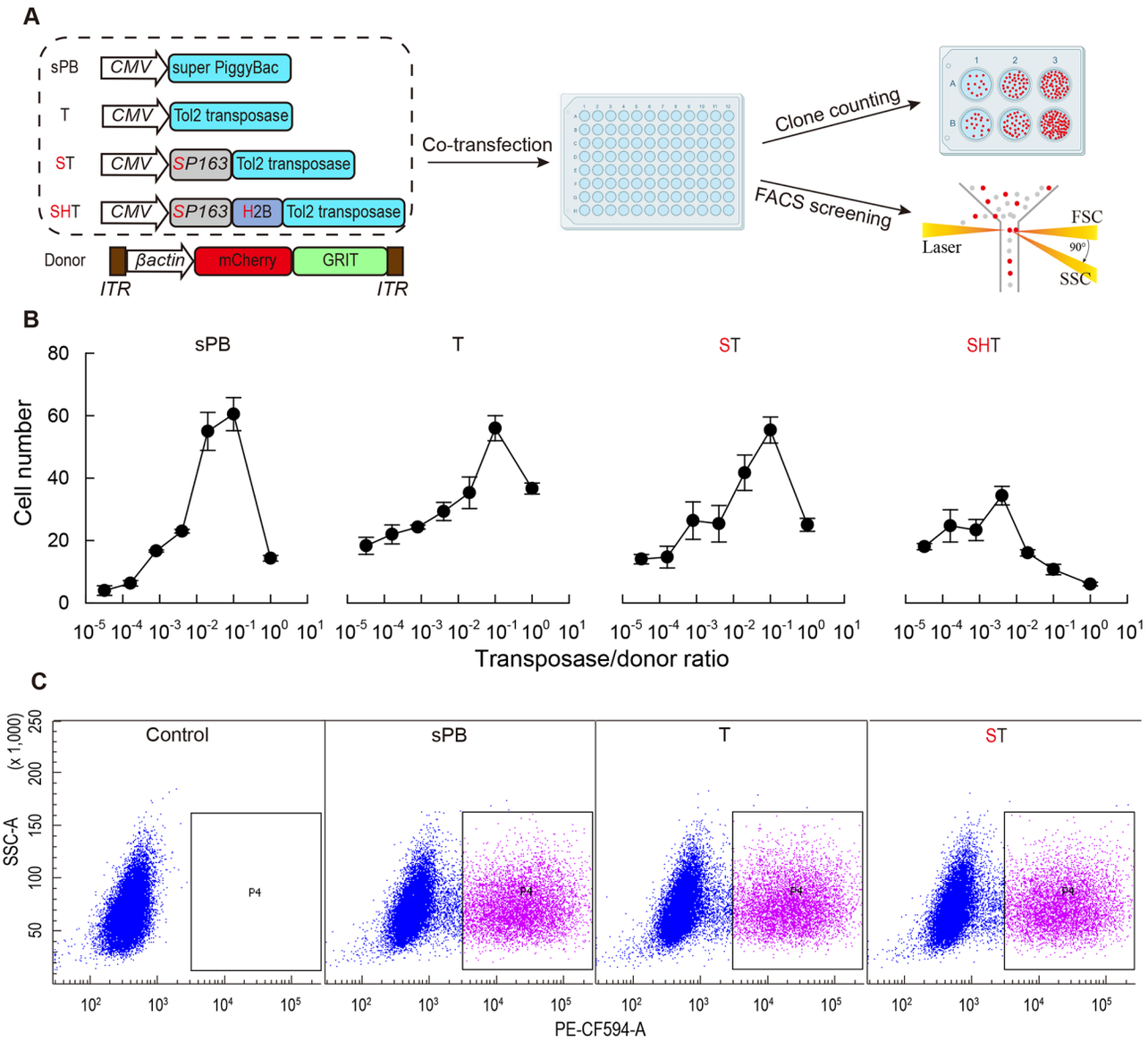

Figure 2 Characterization of different Tol2 transposases in transfected H1299 cells

A: Schematic of transposition efficiency of super PiggyBac (sPB) and various Tol2 transposases. Efficiency was assessed through co-transfection of transposon and donor plasmids, followed by quantification of cell clones and FACS analysis. B: Comparison of sPB with different Tol2 transposases based on efficacy of stable transgene integration. Analysis was conducted at various transposon plasmid dosages while maintaining a constant donor plasmid dosage. C: Quantification of stable integrated cell ratios for sPB, T, and ST at a transposase/donor plasmid ratio of 1:10 using FACS analysis. *n*=3 independent experiments.

the emission of light through the catalysis of luciferin by luciferase, provides non-invasive, real-time monitoring capabilities that are essential for understanding complex biological processes, particularly in studies of deep tissues and sleep. However, the use of most luciferases is limited by their dependence on exogenous substrates. Recent studies have reported that the *Neonothopanus nambi* luciferase (nnLuz) along with several luciferin anabolic enzymes can induce stable luminescence in transgenic yeast and plants (Kotlobay et al., 2018; Mitiouchkina et al., 2020).

We constructed a vector containing the chimeric protein nnLuz-mScarlet (55.8 kDa) and the complete luciferin anabolism pathway and delivered this large payload (24 kb) into zebrafish using either T or SHT transposase mRNA (Figure 4A; Supplementary Figure S4A, B). While no positive cells were observed in the control group (P-T), SHT yielded substantial positive ratios, with 8.91% for Group 2 and 5.88% for Group 3 (Figure 4B, C; Supplementary Figure S4C). Strong RFP signals were detected in the cytoplasm of zebrafish cells, suggesting successful delivery of the entire cargo (Figure 4B). However, no bioluminescence was observed in the zebrafish under dark conditions (data not shown), potentially due to the low quantum yield of nnLuz (Sato et al., 2022) or insufficient luciferin turnover (Kotlobay et al., 2018; Mitiouchkina et al., 2020). In summary, these results demonstrate that a large payload, including the whole luciferin metabolic pathway, can be successfully integrated into the zebrafish genome using enhanced Tol2.

DISCUSSION

In this study, we enhanced Tol2 transposon systems by improving their expression levels and nuclear localization ability, thereby increasing their effectiveness in delivering

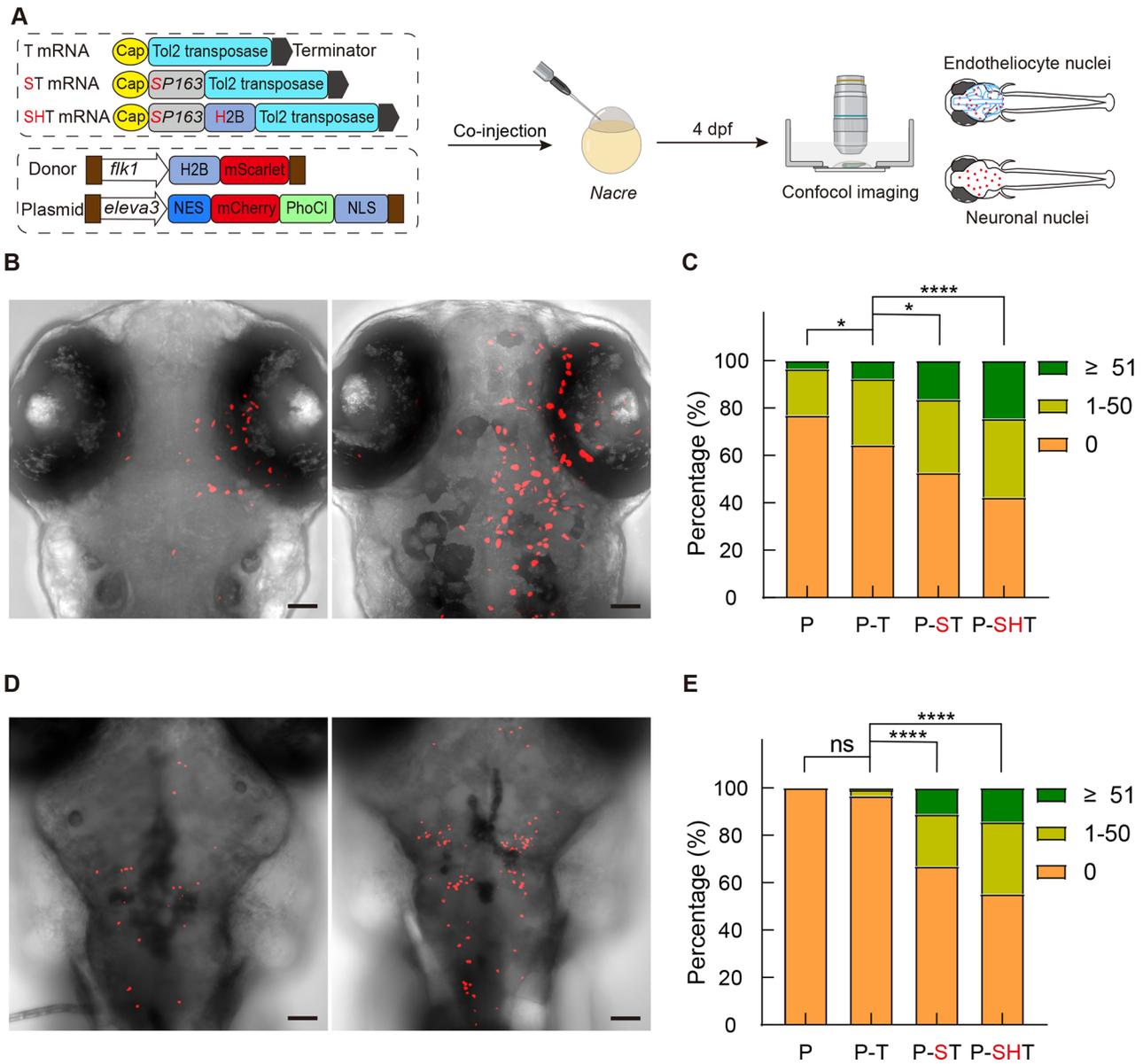

Figure 3 Characterization of transposition efficiency of different Tol2 transposases in zebrafish

A: Schematic of measurement of *in vivo* transposition efficiencies of various Tol2 transposases with two different donor plasmids carrying 8 kb and 14 kb cargo, respectively. dpf: Days post-fertilization. B, C: Representative images of F0 embryos showing patterns of mScarlet-positive endothelial cell nuclei (left, Group 2; right, Group 3) observed in 4 dpf larval zebrafish (B). Categorization was based on number of red fluorescent cells in larval zebrafish: (1) Group 1: No fluorescent cells; (2) Group 2: 1–50 fluorescent cells; (3) Group 3: No less than 51 fluorescent cells. P: Only donor plasmid; P-T, P-ST, P-SHT: Co-injection of donor plasmid with Tol2, SP163-Tol2, and SP163-H2B-Tol2 mRNA, respectively (C). Total fish numbers (*n*) were 117, 104, 110, and 184 for P, P-T, P-ST and P-SHT, respectively. D, E: Representative images (D) and corresponding statistical results (E) depicting Tol2 transposase-dependent transgenesis for labeling neuronal nuclei in 4 dpf larval zebrafish. Total fish numbers (*n*) were 101, 150, 127, and 125 for P, P-T, P-ST and P-SHT, respectively. Scale bars in 3B and 3D: 50 μm. ns: Not significant; *: P<0.05; ****: P<0.0001. Chi-square test for trend.

large cargos. The translational enhancer *SP163*, derived from the 5'-untranslated region of the vascular endothelial growth factor gene (Stein et al., 1998), was employed to increase protein expression levels at the same mRNA level. H2B, a histone protein involved in the chromatin structure of eukaryotic cells, exhibited superior nuclear targeting efficiency. Notably, H2B mRNA, which lacks a hairpin structure (Supplementary Figure S2B), addressed the challenges associated with low Tol2 translation turnover. These strategies could potentially be applied to optimize other transposases and meganucleases to advance transgene research. Additionally, we identified a previously unreported monopartite NLS peptide, which may contribute to the partial nuclear localization of the Tol2 protein and its ability to integrate DNA cargos into the genome within nuclei.

We also found that Tol2 and its ST variant exhibited gene integration efficiency in cultured cells comparable to the widely used sPB system, and efficiently delivered large payloads into zebrafish using ST and SHT mRNA. These findings position Tol2 transposons as viable alternatives for delivering large DNA cargos in plasmids, especially where multiple genetic elements need to be incorporated, such as the whole luciferin synthetic pathway for bioluminescence. Despite challenges in detecting nnLuz luminescence in transgenic zebrafish, further

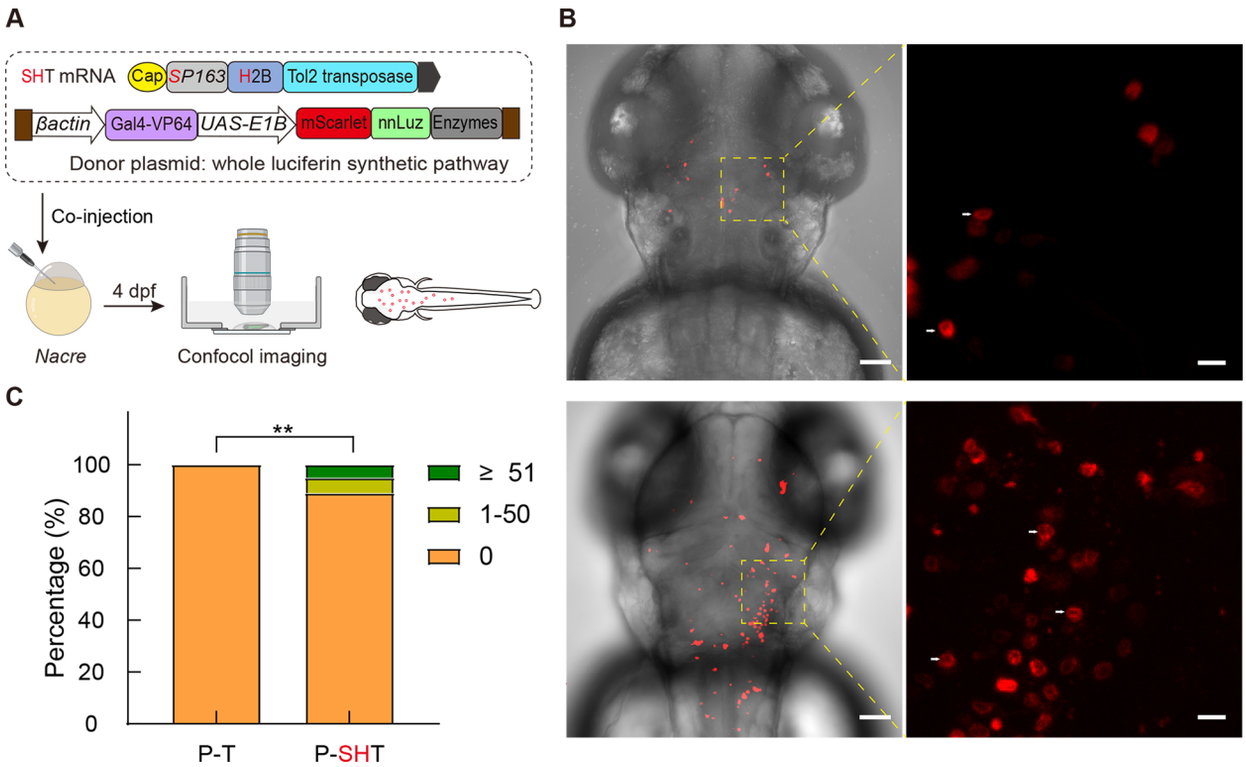

Figure 4 Transposition of whole luciferin metabolic pathway in zebrafish

A: Schematic of measurement of *in vivo* transposition efficiencies of modified Tol2 transposases with a donor plasmid carrying the whole luciferin synthetic pathway (24 kb). dpf: Days post-fertilization. B, C: Confocal images of F0 embryos showing patterns of mScarlet-positive cell cytoplasm (top, Group 2; bottom, Group 3) in 4 dpf larval zebrafish. Enlarged views of boxed areas are shown on the right (B). Categorization was based on number of red fluorescent cells in larval zebrafish. P-T: Tol2 mRNA (*n*=103), P-SHT: SP163-H2B-Tol2 mRNA (*n*=119) (C). Scale bars in 4B: left, 50 μm; right, 10 μm. **: *P*<0.01. Chi-square test for trend.

improvements in enzyme activity (Beregovaya et al., 2021) or synthetic pathways (Shakhova et al., 2024) may unlock its full potential for cellular processes *in vivo*. Furthermore, Tol2 could facilitate the integration of multivalent chimeric antigen receptors into T cells, offering new avenues in immunotherapy for targeting solid tumors with neoantigens (Riley et al., 2019). In addition, the ST and SHT systems could also be applied to bacterial artificial chromosome (BAC) vectors to increase the transgene efficiency of DNA fragments up to 200 kb (Sandoval-Villegas et al., 2021).

In conclusion, the improved Tol2 transposon system holds great promise for advancing transgenic experiments involving large DNA payloads, contributing to the construction of transgenic zebrafish lines, facilitating metabolic pathway engineering, and supporting the development of novel cell therapies.

SUPPLEMENTARY DATA

Supplementary data to this article can be found online.

COMPETING INTERESTS

The authors declare that they have no competing interests.

AUTHORS' CONTRIBUTIONS

R.T. designed and conceived the project. P.C.W., R.T., and H.D. performed experiments, analyzed the data, created figures, and wrote the draft. R.T., R.X., and J.L.D. revised the manuscript. All authors read and approved the final version of the manuscript.

ACKNOWLEDGMENTS

We appreciate the comments from Dr. Jia Li (Center for Excellence in Brain Science and Intelligence Technology). We thank Ji-Wen Bu for secretarial assistance (Center for Excellence in Brain Science and Intelligence Technology). We thank the Chemical Biology Core Facility and Molecular Biology Core Facility from the CAS Center for Excellence in Molecular Cell Science for technical support.

REFERENCES

Abdelfattah AS, Kawashima T, Singh A, et al. 2019. Bright and photostable chemigenetic indicators for extended in vivo voltage imaging. Science, 365(6454): 699–704.

Bak RO, Porteus MH. 2017. CRISPR-mediated integration of large gene cassettes using AAV donor vectors. Cell Reports, 20(3): 750–756.

Balciunas D, Wangensteen KJ, Wilber A, et al. 2006. Harnessing a high cargo-capacity transposon for genetic applications in vertebrates. PLoS Genetics, 2(11): e169.

Beregovaya KA, Myshkina NM, Chepurnykh TV, et al. 2021. Rational design and mutagenesis of fungal luciferase from *Neonothopanus nambi*. *Doklady Biochemistry and Biophysics*, **496**(1): 14–17.

Chiang CY, Ligunas GD, Chin WC, et al. 2020. Efficient nonviral stable transgenesis mediated by retroviral integrase. Molecular Therapy - Methods & Clinical Development, 17: 1061–1070.

Freeman J, Vladimirov N, Kawashima T, et al. 2014. Mapping brain activity at scale with cluster computing. Nature Methods, 11(9): 941–950.

Grabher C, Joly JS, Wittbrodt J. 2004. Highly efficient zebrafish transgenesis mediated by the meganuclease I-scei. Methods in Cell Biology, 77: 381–401.

Huang X, Guo HF, Tammana S, et al. 2010. Gene transfer efficiency and genome-wide integration profiling of *Sleeping Beauty, Tol2*, and *PiggyBac* transposons in human primary T cells. Molecular Therapy, 18(10):

1803–1813.
Jumper J, Evans R, Pritzel A, et al. 2021. Highly accurate protein structure prediction with AlphaFold. Nature, 596(7873): 583–589.
Kawakami K. 2007. *Tol2*: a versatile gene transfer vector in vertebrates. *Genome Biology*, **8 Suppl 1**(Suppl 1): S7.
Kosugi S, Hasebe M, Tomita M, et al. 2009. Systematic identification of cell cycle-dependent yeast nucleocytoplasmic shuttling proteins by prediction of composite motifs. Proceedings of the National Academy of Sciences of the United States of America, 106(25): 10171–10176.
Kotlobay AA, Sarkisyan KS, Mokrushina YA, et al. 2018. Genetically encodable bioluminescent system from fungi. Proceedings of the National Academy of Sciences of the United States of America, 115(50): 12728–12732.
Kozak M. 1986. Influences of mRNA secondary structure on initiation by eukaryotic ribosomes. Proceedings of the National Academy of Sciences of the United States of America, 83(9): 2850–2854.
Li J, Zhang BB, Ren YG, et al. 2015. Intron targeting-mediated and endogenous gene integrity-maintaining knockin in zebrafish using the CRISPR/Cas9 system. Cell Research, 25(5): 634–637.
Mashel TV, Tarakanchikova YV, Muslimov AR, et al. 2020. Overcoming the delivery problem for therapeutic genome editing: current status and perspective of non-viral methods. Biomaterials, 258: 120282.
Mitiouchkina T, Mishin AS, Somermeyer LG, et al. 2020. Plants with genetically encoded autoluminescence. Nature Biotechnology, 38(8): 944–946.
Riley RS, June CH, Langer R, et al. 2019. Delivery technologies for cancer immunotherapy. Nature Reviews Drug Discovery, 18(3): 175–196.
Sandoval-Villegas N, Nurieva W, Amberger M, et al. 2021. Contemporary transposon tools: a review and guide through mechanisms and applications of *Sleeping Beauty, piggyBac* and *Tol2* for genome engineering. International Journal of Molecular Sciences, 22(10): 5084.
Sato W, Rasmussen M, Deich C, et al. 2022. Expanding luciferase reporter systems for cell-free protein expression. Scientific Reports, 12(1): 11489.
Shakhova ES, Karataeva TA, Markina NM, et al. 2024. An improved pathway for autonomous bioluminescence imaging in eukaryotes. Nature Methods, 21(3): 406–410.
Silva G, Poirot L, Galetto R, et al. 2011. Meganucleases and other tools for targeted genome engineering: perspectives and challenges for gene therapy. Current Gene Therapy, 11(1): 11–27.
Stein I, Itin A, Einat P, et al. 1998. Translation of vascular endothelial growth factor mRNA by internal ribosome entry: implications for translation under hypoxia. Molecular and Cellular Biology, 18(6): 3112–3119.
Suster ML, Kikuta H, Urasaki A, et al. 2009. Transgenesis in zebrafish with the *Tol2* transposon system. *In*: Cartwright EJ. Transgenesis Techniques: Principles and Protocols. Totowa: Humana, 41–63.
Tambuyzer E, Vandendriessche B, Austin CP, et al. 2020. Therapies for rare diseases: therapeutic modalities, progress and challenges ahead. Nature Reviews Drug Discovery, 19(2): 93–111.
Tao RK, Wang K, Chen TL, et al. 2023. A genetically encoded ratiometric indicator for tryptophan. Cell Discovery, 9(1): 106.
Tao RK, Zhao YZ, Chu HY, et al. 2017. Genetically encoded fluorescent sensors reveal dynamic regulation of NADPH metabolism. Nature Methods, 14(7): 720–728.
Tsukahara T, Iwase N, Kawakami K, et al. 2015. The *Tol2* transposon system mediates the genetic engineering of T-cells with CD19-specific chimeric antigen receptors for B-cell malignancies. Gene Therapy, 22(2): 209–215.
Urasaki A, Asakawa K, Kawakami K. 2008. Efficient transposition of the *Tol2* transposable element from a single-copy donor in zebrafish. Proceedings of the National Academy of Sciences of the United States of America, 105(50): 19827–19832.
Yuen G, Khan FJ, Gao SJ, et al. 2017. CRISPR/Cas9-mediated gene knockout is insensitive to target copy number but is dependent on guide RNA potency and Cas9/sgRNA threshold expression level. Nucleic Acids Research, 45(20): 12039–12053.
Zhang W, Lohman AW, Zhuravlova Y, et al. 2017. Optogenetic control with a photocleavable protein, PhoCl. Nature Methods, 14(4): 391–394.
Zhang WM, Golynker I, Brosh R, et al. 2023. Mouse genome rewriting and tailoring of three important disease loci. Nature, 623(7986): 423–431.